Passivation Coating on Electrospun Copper Nanofibers for Stable Transparent Electrodes

Po-Chun Hsu,[†] Hui Wu,[†] Thomas J. Carney,[†] Matthew T. McDowell,[†] Yuan Yang,[†] Erik C. Garnett,[†] Michael Li,[†] Liangbing Hu,[†,§] and Yi Cui[†,‡,*]

[†]Department of Materials Science and Engineering, Stanford University, Stanford, California 94305, United States and [‡]Stanford Institute for Materials and Energy Sciences, SLAC National Accelerator Laboratory, 2575 Sand Hill Road, Menlo Park, California 94025, United States. [§]Present address: Department of Materials Science and Engineering, University of Maryland, College Park, MD 20742.

ABSTRACT

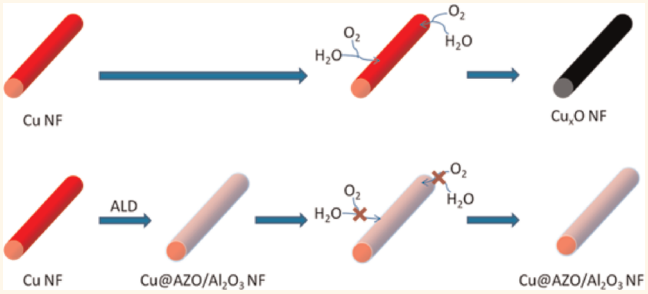

Copper nanofiber networks, which possess the advantages of low cost, moderate flexibility, small sheet resistance, and high transmittance, are one of the most promising candidates to replace indium tin oxide films as the premier transparent electrode. However, the chemical activity of copper nanofibers causes a substantial increase in the sheet resistance after thermal oxidation or chemical corrosion of the nanofibers. In this work, we utilize atomic layer deposition to coat a passivation layer of aluminum-doped zinc oxide (AZO) and aluminum oxide onto electrospun copper nanofibers and remarkably enhance their durability. Our AZO—copper nanofibers show resistance increase of remarkably only 10% after thermal oxidation at 160 °C in dry air and 80 °C in humid air with 80% relative humidity, whereas bare copper nanofibers quickly become insulating. In addition, the coating and baking of the acidic PEDOT:PSS layer on our fibers increases the sheet resistance of bare copper nanofibers by 6 orders of magnitude, while the AZO—Cu nanofibers show an 18% increase.

KEYWORDS: transparent electrodes · electrospinning · metal nanofibers · atomic layer deposition · surface passivation

Transparent electrodes are widely used in optical-electronic devices such as solar cells, displays, organic light-emitting diodes (OLED), and touch screens.[1−3] While the performance of a transparent electrode is generally determined by the sheet resistance (R_s) and the transparency (T), other properties also profoundly affect the applicability of the material as a transparent electrode. For instance, durability against chemical corrosion and mechanical stress are key characteristics for practical applications. Although the conventional transparent electrode material, tin-doped indium oxide (ITO), possesses high transparency and conductivity, ITO is inherently brittle and therefore not stable under mechanical stress. Indeed, the sheet resistance of ITO thin film increases dramatically when the strain exceeds 0.03 due to crack formation.[4] This strain-induced failure not only compromises the reliability of ITO but also limits its applicability on flexible substrates. Moreover, the cost of manufacturing ITO-based transparent electrodes is directly proportional to the cost and scarcity of indium. In 2010, the price of elemental indium reached $550 per kilogram, and given the abundance of transparent electrodes in modern optical-electronic devices, the cost of indium is only expected to increase due to both supply and demand consequences.[5] Thus, it is of vital importance to find an alternative material and engineer its nanostructure to improve its performance and reduce its cost in an effort to replace traditional ITO. Recently, researchers fabricated transparent electrodes from conductive polymers,[6] carbon nanotubes,[7] graphenes,[8] metal nanowires,[9] and nanofibers[10] and evaluated their performance. Conductive polymers, carbon nanotubes, and graphene demonstrate better flexibility than ITO, but with sheet resistance typically more than 100 Ω/sq at 80% transparency,[3] which is inferior to conventional ITO in modern devices such as solar cells and OLEDs. Although the conductivity can be further enhanced by proper doping, the subsequent degradation of sheet resistance reveals the instability of this doping method.[11] Metal nanowires, generally made of silver, have low R_s/T ratio comparable with ITO

* Address correspondence to yicui@stanford.edu.

Received for review February 25, 2012 and accepted May 1, 2012.

Published online May 01, 2012
10.1021/nn300844g

thin films,[12] but the high price of silver remains an obstacle for future large-scale use. Recently, we demonstrated the novel idea of electrospinning copper nanofibers as a transparent electrode to achieve excellent transparency and sheet resistance with relatively cheap material and processing. This technique shows great potential in replacing ITO as the conventional transparent electrode; however, due to the large surface area of nanofibers, the lack of stability of copper against thermal oxidation and chemical corrosion remains a concern. For example, in our early study, the performance of electrospun Cu nanofibers degrades after it is employed in an organic photovoltaic cell, mainly due to the acidic poly(3,4-ethylenedioxythiophene):poly(styrenesulfonate) (PEDOT:PSS), a commonly used polymeric hole conductor in organic photovoltaic cells. The corrosion and oxidation can decrease the effective cross section area of Cu nanofibers and cause the conductivity to diminish.[10] Given the high performance and low cost of electrospun Cu nanofibers as a transparent electrode, it is crucial to enhance the chemical stability of copper nanofibers to further strengthen its application in practical devices. In this paper, we sought to address this problem by constructing a conformal passivation coating on the outside of copper nanofibers. We expect that the passivation coating developed here can also be extended to other nanowire network technology.

Atomic layer deposition (ALD) features in its conformal coating in comparison with other deposition techniques.[13] By purging precursors and adsorbing molecular monolayers in sequence, the growth rate of a thin film can be precisely limited to only one molecular layer at one time. Owing to this self-limiting mechanism, ALD can achieve a highly conformal and dense metal oxide coating without pinholes even on surfaces with high aspect ratio[14] or high curvature.[15] These features make ALD an ideal tool for building passivation layers on nanostructured materials. Herein, we introduce the ALD coatings on electrospun Cu nanofibers for the purpose of enhancing the chemical resistance against corrosion and oxidation. In our study, the profound distinction of stability between bare Cu nanofibers and AZO−Cu nanofibers clearly proves the effectiveness of our ALD-based protection technique, which can extend the applicability of an electrospun Cu nanofiber transparent electrode.

RESULTS AND DISCUSSION

Cu Nanofiber Synthesis and ALD Coating. Electrospinning is one of the most facile and cost-effective techniques to synthesize ultralong one-dimensional nanomaterials due to its large yield and relatively cheap equipment.[16] Typically, a viscous polymer solution is loaded inside a syringe and pushed out by a syringe pump. As a droplet of the solution appears at the needle tip, an electrical field is applied between the needle and the grounded substrate. When the electrical force exerted on the solution overcomes the surface tension, the spherical droplet become cone-shaped, which is known as Taylor cone, and nanofibers are expelled from the tip of the needle.[17,18] In addition to fabricating polymer nanofiber networks, electrospinning has been also employed as a method to produce carbon,[19] metal,[20] ceramics,[21] and composite nanofibers.[22] Recently, we introduced electrospinning to fabricate Cu nanofiber webs as a transparent electrode material.[10] The high ratio of transmittance to sheet resistance, excellent flexibility, and simple experimental setup are advantageous for numerous transparent electrode applications. However, the sheet resistance of Cu nanofibers gradually increases after being exposed in air.[10] Unlike aluminum oxide which is capable of passivating the underlying aluminum, copper oxide grows as an island and then coalesces into the film which tends to have pinholes and microcracks.[23] Thus the oxidation can often spread through the entire copper nanofiber and cause a significant drop in conductivity. Furthermore, the large surface area of copper nanofibers compounds the problem of conductivity loss as compared to a bulk or thin film of Cu because the large surface area provides more sites for Cu_xO island formation. To solve this reliability problem, we proposed three routes of metal passivation: noble metal coating, alloying, and oxide layer coating. Among those routes, noble metals, such as gold or platinum, are too expensive, and therefore, the advantage of making a cheap transparent electrode solely from cheap, earth-abundant copper is sacrificed for performance. Alloying employs a different metal to form a dense and continuous oxide layer for surface passivation; however, transparent electrodes require high conductivity, which limits the alloying concentration and therefore cannot guarantee continuous coating at nanoscale. Consequently, coating a uniform, dense, and inert oxide layer to protect Cu nanofibers is the most feasible and effective method for corrosion and oxidation prevention.

The principle of our experiment is illustrated in Figure 1a. We employ the passivation layer on electrospun Cu nanofibers and compare the reliability with bare Cu nanofibers. This passivation layer can shield the Cu nanofibers from oxidation and corrosion and thus maintain its electrical and optical performance in harsh environments. We choose the ALD process as our coating method for its capability of creating a conformal layer, as compared with other coating techniques, such as sputtering, evaporation, and chemical vapor deposition (CVD). The self-limiting, surface-controlled growth mechanism of ALD allows only one molecular layer to coat onto Cu nanofibers at any single time; thus, the film growth rate is identical across the surface area of the Cu nanofibers. For transparent electrode applications, we chose AZO as our protecting

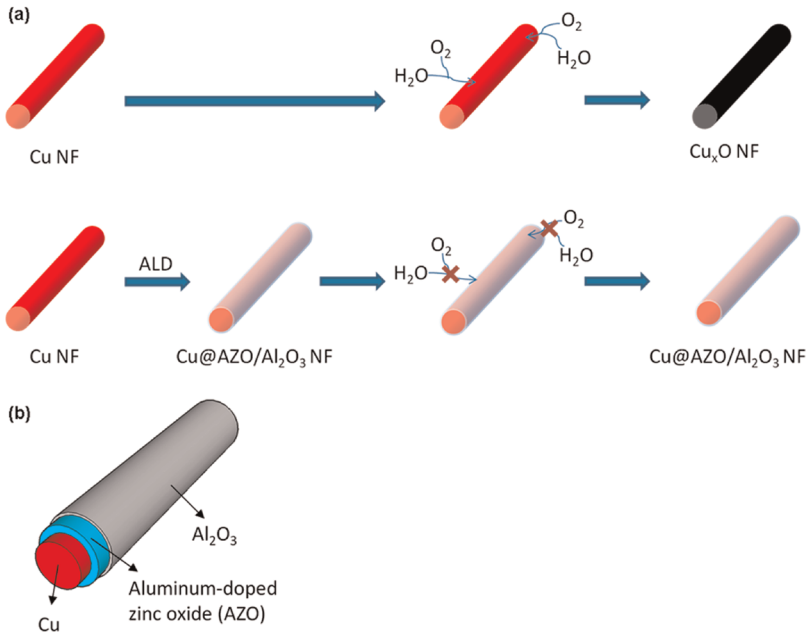

Figure 1. (a) Schematic of AZO–Cu nanofiber preparation and comparison with bare Cu nanofiber in terms of oxidation resistance. Because of the passivation of the AZO/Al_2O_3 layer, the core Cu nanofiber is not subjected to oxidation and therefore can maintain its high conductivity. (b) Cartoon (not to scale) of the Cu@AZO/Al_2O_3 nanofiber.

oxide layer due to its transparency, conductivity, and low cost. However, one possible drawback of AZO coating is its low chemical stability against acid corrosion. Anticipating this potential problem, a 1 nm Al_2O_3 layer was coated onto AZO to improve its acid resistance without sacrificing its previously mentioned advantages. The core–shell structure is illustrated in Figure 1b. Although we expect some of the Al to diffuse into the AZO film, nevertheless, pure Al_2O_3 is proved to exist on the outside by our experimental chemical corrosion analysis. It is also worth noting that Al_2O_3 and AZO share the same precursors and experimental setup during ALD, which simplifies this dual-layer process. Moreover, the hydroxyl groups on the surface of the AZO layer are reactive with the organoaluminum precursors, namely, trimethylaluminum. These hydroxyl groups are able to provide efficient nucleation and ensure that the coalescence of nuclei is good enough for a conformal coating, which is not the case if the ultrathin Al_2O_3 layer is deposited directly onto Cu nanofibers.[24]

Morphology and Chemical Analysis. The morphology of Cu nanofibers and AZO–Cu nanofibers was characterized by scanning electron microscopy (Figure 2a,b). The fusion at the junctions, which remarkably decreases the resistance, can be observed in both samples. In AZO–Cu nanofibers, the junctions are reinforced by the AZO/Al_2O_3 layer and hence may further improve the conductivity. Furthermore, the coating holds Cu nanofibers to the glass substrate stronger than bare Cu nanofibers and therefore improves the mechanical durability. To demonstrate this phenomenon, we applied Scotch adhesive tape on both

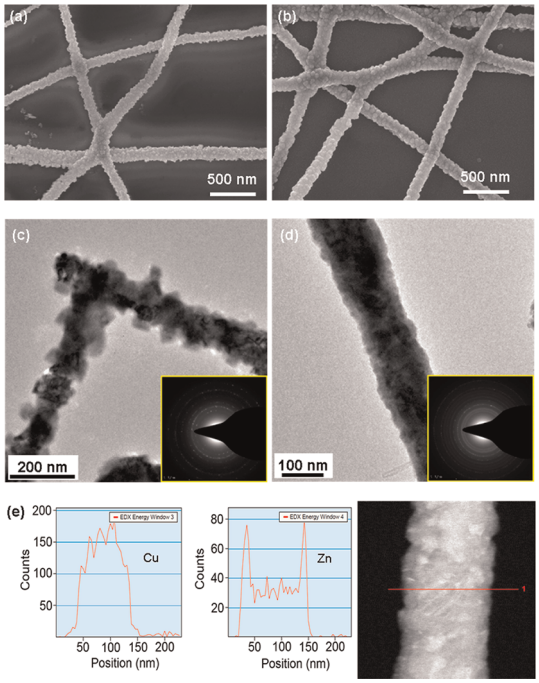

Figure 2. Characterization of bare Cu and AZO–Cu nanofibers: SEM images of bare Cu (a) and AZO–Cu (b) nanofibers exhibit fusion at junctions. TEM images and diffraction patterns (insets) of Cu nanofibers (c) and AZO–Cu (d) nanofibers. EDS line scan profile and the corresponding dark-field image of Cu/AZO/Al_2O_3 nanofiber (e).

samples and then peeled off the tape. All of the bare Cu nanofibers were removed by the tape, and the sample became insulating (>20 MΩ), whereas AZO–Cu nanofiber sheet resistance only increased by a factor of 6. TEM and energy-dispersive X-ray spectroscopy (EDS)

were employed to characterize the phases, crystallinity, and chemical composition of the nanofibers. Figure 2c shows the polycrystalline nature of Cu nanofibers. The diffraction pattern indicates that the nanofibers are composed of not only Cu but also Cu_2O, which means the native oxide has already formed during the exposure in air. It is also the formation of Cu_2O which explains the irregular grains on the surface, as shown in Figure 2c. This result microscopically demonstrates that Cu nanofibers are inherently vulnerable to atmospheric oxidation. As for AZO−Cu, only face-centered cubic (fcc) Cu and ZnO are found in the sample (Figure 2d inset). Taking the chemical activity of bare Cu nanofibers into account, it is reasonable to infer that, if Cu nanofibers are stored in air for too long before ALD passivation, Cu_2O should be found in the sample, as well. Consequently, it is critical to reduce the exposure time of Cu nanofibers with air in order to maximize the conductivity of the fibers.

In the TEM image of AZO−Cu nanofibers (Figure 2d), the contrast line along the axial direction is the boundary between Cu and AZO/Al_2O_3 coating. The thickness of the coating is approximately 25 nm, and the diameter of core Cu nanofiber is around 100 nm. EDS line scan (Figure 2e) is also used to examine the elemental distribution. The two peaks at the edges of the Zn concentration profile clearly show the shell structure of the AZO/Al_2O_3 layer. By measuring the width of the peak, we are able to confirm the thickness of the AZO/Al_2O_3 layer to be the same as observed in microscope images.

Optical and Electronic Property. A major concern surrounding our method is how the resistance of AZO/Al_2O_3 influences the transmittance and sheet resistance of Cu nanofiber electrodes. To examine this, we patterned electrical contacts by gold evaporation on the samples for electrical measurement. Upon comparing the sheet resistance both before and after ALD, we find the resistance to be the same at 47.1 Ω/sq. This indicates the AZO/Al_2O_3 layer does not block the electrical current, and the ALD process itself does not degrade the conductivity of Cu nanofibers. It is worth noting that the conductance of nanostructure transparent electrodes is typically attributed to percolation theory, which assumes that only nanofibers which form a continuous pathway between electrical contacts contribute to the conductance, while dead-end nanofibers do not.[25] Although the sheet resistance does not change here, it is reasonable to argue that the implementation of AZO can connect those dead-end Cu nanofibers together and enable them to complete the electrical circuit and possibly increase the total conductance. The thickness of Al_2O_3 layer is only 1 nm, which is thin enough for carrier tunneling, and the AZO layer is also thin and inherently conductive, so carrier transport from the active layer to the transparent electrode will also not be blocked. Moreover, optical measurements (Figure 3a) show less than a 1% decrease in transmittance throughout the entire visible light wavelength range. Thus, we conclude the choice of transparent AZO and ultrathin Al_2O_3 as our coating has no effect on the performance of Cu nanofibers.

Thermal Oxidation Stability. AZO/Al_2O_3-coated Cu nanofibers exhibit significant enhancement of thermal oxidation resistance. Cu nanofibers were tested at 80, 120, and 160 °C. To show the effect of degradation, the sheet resistance was normalized using its original value. Figure 3b shows that all bare Cu nanofibers become more insulating than their AZO-coated counterpart. In particular, the sheet resistance of bare Cu nanofibers increases dramatically at 120 and 160 °C. The AZO−Cu nanofibers, on the other hand, show increases of sheet resistance of only 10%, even at temperatures as high as 160 °C for 8 h, as compared to the bare Cu nanofibers which become insulating (>20 MΩ) after only 40 min. This profound difference in thermal oxidation stability demonstrates the effectiveness of the AZO/Al_2O_3 layer in enhancing the durability of Cu nanofiber transparent electrodes for practical application. As shown in Figure 3c, after baking the fibers at 120 °C for 7 h, the bare Cu nanofibers become light brown, suggesting the oxidation of Cu, while the AZO−Cu nanofibers remain red, indicating a lack of oxidation. At ambient temperature, the electrical performance of Cu nanofibers degrades relatively slowly (Figure 3d), but the sheet resistance still increases 53% after 25 days. The two sudden increases of sheet resistance might correspond to the change in ambient humidity because water vapor can greatly accelerate the oxidation of copper metal.[26] Transmission electron microscopy characterization (Figure 3e) shows that Cu nanofibers are oxidized into Cu_2O after baking at 120 °C for more than 3 h, during which the sheet resistance rises to more than 20 MΩ. We find no fcc Cu inside the sample, although we do observe unidentified diffraction peaks which are probably due to the mixture of copper carbonate and copper hydroxide, the two main products of copper oxidation in air. In contrast, for AZO−Cu nanofibers, the electron image and diffraction pattern remain the same as before heating (Figure 3f), indicating our thermal oxidation does not affect the AZO/Al_2O_3-protected Cu nanofibers. EDS scanning profile (Figure S1 in Supporting Information) verifies that the core−shell structure does not change after thermal treatment. Therefore, we conclude that Cu nanofibers are preserved inside the AZO/Al_2O_3 layer and maintain their high conductivity.

After oxidation, most of the oxidized Cu nanofibers retain their polycrystallinity and morphology rather than transforming into Cu_2O nanotubes as in the case of Cu single-crystalline nanowires.[27] The formation of CuO or Cu_2O nanotubes is primarily due to the Kirkendall effect, which arises from the difference in

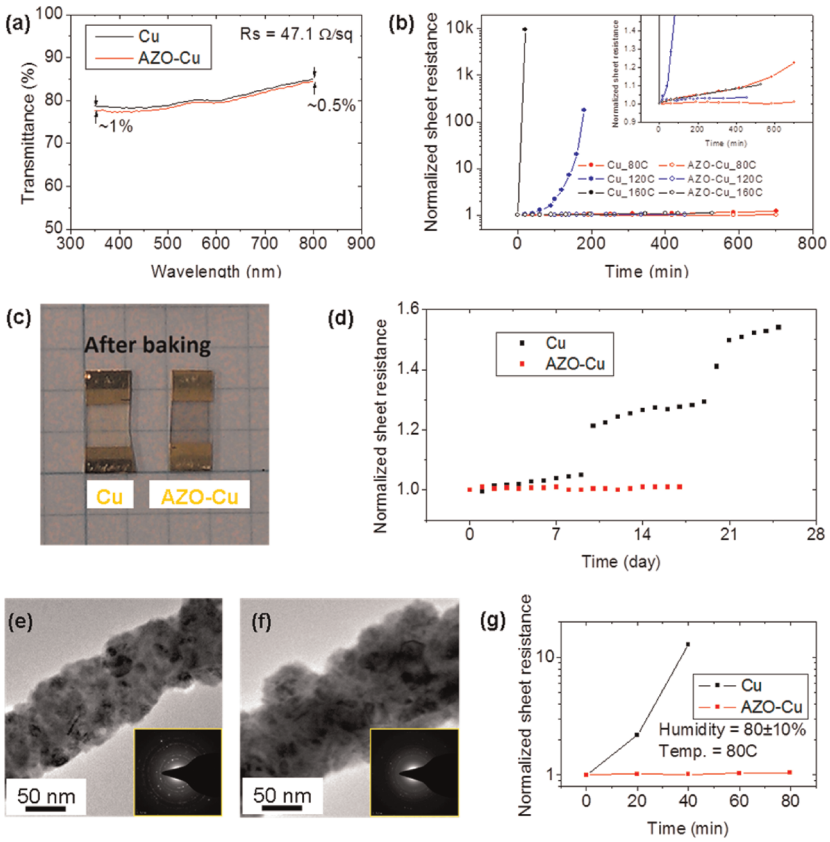

Figure 3. (a) Transmittance of electrospun Cu nanofibers before and after ALD. Note that the transmittance is measured from the same sample, and sheet resistance does not change after the ALD process. (b) Normalized sheet resistance *versus* baking time at 80, 120, and 160 °C. Solid circles refer to bare Cu nanofibers, and hollow circles represent AZO−Cu nanofibers. In the case of bare Cu nanofibers at 120 and 160 °C, the resistance exceeds multimeter limit (20 MΩ) in the end. (c) Photos of Cu and AZO−Cu nanofibers after baking in dry air. The color change reveals the oxidation of Cu nanofibers. The edge length of one grid cell is 0.2 in. (d) Sheet resistance change *versus* time under ambient temperature and atmosphere sheet resistance. (e,f) TEM images and diffraction patterns of Cu and AZO−Cu nanofibers, respectively. (g) Humidity test data.

diffusivity. Since copper diffuses faster than oxygen in its oxide phase, voids will form in the copper region. In a one-dimensional nanostructure, the accumulation and coalescence of voids eventually forms a hollow structure inside and becomes a CuO nanotube. The reason why Kirkendall effect is not observed in electrospun Cu nanofibers lies in the crystallinity of our fibers. For the electrospun polycrystalline Cu nanofibers, oxidation begins at the grain boundary rather than the surface of nanofibers because of the dominating diffusivity along the grain boundary. SEM and TEM images show that the grain size of the Cu nanofiber is less than 40 nm. As a result, vacancies tend to diffuse to the grain boundaries, and the vacancy concentration inside the grain will not be high enough to form voids or at least not experimentally distinguishable under TEM.

The influence of humidity on sheet resistance increase was also tested. As shown in Figure 3g, the temperature and relative humidity were controlled at 80 °C and 80 ± 10%, respectively. Under this environment, bare Cu nanofibers became insulating in less than 60 min, due to the fact that a large amount of water vapor molecules is adsorbed onto the surface and accelerates the oxidation.[28] In comparison with testing in 80 °C dry air (Figure 3b) in which the sheet resistance of bare Cu nanofibers increases 22% after 700 min, humidity does play an important role in Cu thermal oxidation. As for AZO/Al_2O_3-protected Cu nanofibers, the sheet resistance increases by only 4.6% in humid air and 1% in dry air. Although the AZO−Cu nanofibers are still affected by the humid air, the passivation layer still demonstrates a significant improvement in performance as compared to the extremely high oxidation rate of bare Cu nanofibers in a humid environment.

Chemical Corrosion Stability. For transparent electrode applications, the chemical stability against an acidic environment is of great interest. In particular, the corrosion of a transparent electrode by acidic PEDOT:PSS can degrade the interface and thus reduce the performance of the transparent electrode.[29] This phenomenon is compounded in Cu nanofibers as compared to ITO because of the greater chemical activity of Cu. Moreover, the baking process can accelerate the oxidation of the nanofibers, which results in a dramatic increase of sheet resistance. To test the corrosion resistance of our fibers, we immersed the bare Cu and AZO−Cu nanofibers into aqueous solution of

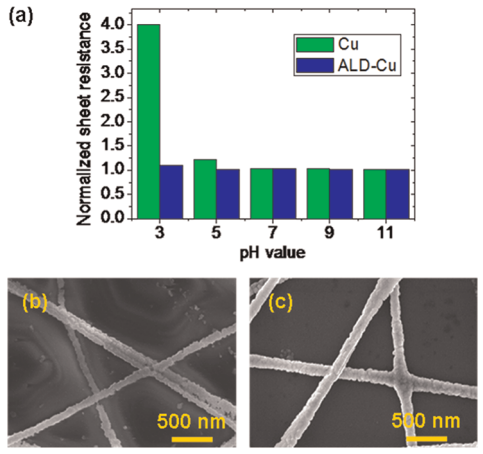

Figure 4. (a) Normalized sheet resistance after acid or base etching. (b,c) SEM images of bare Cu and AZO−Cu nanofiber after etching in acidic (pH 3) solution for 1 min.

various pH values for 1 min (Figure 4a). In the acidic solutions, the AZO−Cu nanofibers exhibit remarkable resistance against corrosion as compared to the poor performance of the bare Cu fibers; while in DI water and basic solution, the sheet resistance of both Cu and AZO−Cu nanofibers does not change significantly. SEM images (Figure 4b,c) also demonstrate that bare Cu nanofibers suffer severe etching, which shrinks the effective cross section area on surface active sites or even breaks the entire nanofiber, whereas AZO−Cu nanofibers do not show morphology change after etching, further confirming the stability of the AZO/Al_2O_3 passivation layer.

Besides the testing under various pH environments, the impact of the PEDOT:PSS coating process is also investigated. PEDOT:PSS aqueous solution (pH ~3) was spin-coated onto the nanofibers on glass substrates followed by 120 °C baking in air for 15 min. The sheet resistance of Cu nanofibers increased by a factor of 5.26×10^6, whereas AZO−Cu nanofibers only showed an 18% increase. It is important to note that the nanofibers were subjected to a relatively harsh environment through this test. In practice, this degradation caused by PEDOT:PSS can be mitigated by choosing a pH-neutral PEDOT:PSS[30] or baking in vacuum to avoid subsequent thermal oxidation, and thus AZO−Cu nanofibers should be able to withstand the corrosion by the PEDOT:PSS coating process to an even higher level.

CONCLUSIONS

In summary, we demonstrated that using an ALD technique to coat an AZO/Al_2O_3 passivation layer onto electrospun Cu nanofibers can significantly enhance the fibers' stability against oxidation and corrosion. This approach hinges on the chemical stability of the outer Al_2O_3 ultrathin film and the conductivity and transparency of AZO to solve the reliability problem of a Cu nanostructure-based transparent electrode. This passivation layer has a remarkable effect in preventing Cu nanofibers from thermal oxidation at high temperature of up to 160 °C in dry air and 80 °C in humid air. After coating the nanofibers with PEDOT:PSS, the sheet resistance of AZO−Cu nanofibers increases only 18%, while bare Cu nanofibers increase by 5.26×10^6. Given the extraordinary performance and cost-effectiveness of electrospun Cu nanofibers as transparent electrodes, this passivation method provides a critical advantage for Cu nanofibers to replace ITO in industry and commercial use. In addition, our study shows that building an ALD passivation layer on material surfaces is also a general and effective route to improve the chemical stabilities of other nanostructured metals.

METHODS

Electrospinning. The polymer solution was prepared by dissolving polyvinyl alcohol (PVA) (avg. M_w = 95 000 g/mol, Acros) in distilled water with a concentration of 10 wt %. The PVA solution was stirred and heated at 85 °C for 3 h until a clear and uniform solution was formed. Copper(II) acetate monohydrate ($CuAc_2$) (Aldrich) was added into the PVA solution to a concentration of 10 wt %. The solution was again stirred and heated at 85 °C for 3 h forming a turquoise gel solution. After the $CuAc_2$ dissolved, the saturated solution was cooled to room temperature and held still for 1 day. The $CuAc_2$/PVA solution was electrospun using a 1 mL syringe with a 22 gauge, blunt, stainless steel needle, flow rate of 0.1 mL/h (KDS200, KD Scientific Inc.), and applied voltage of 0.6 kV/cm (Gamma High Voltage Research). The collector used for the electrospinning process was aluminum foil with a glass slide on top. These parameters produced a Taylor cone at the needle tip, although slight flow rate adjustment was needed to maintain a stable Taylor cone.

Calcination and Reduction of Nanofibers. The $CuAc_2$/PVA nanofibers were calcinated using the tube furnace (Lindberg/Blue M) under a nitrogen/oxygen gas mixture at 1 atm. The flow rate of nitrogen and oxygen was 40 and 6 sccm, respectively. The nanofibers were then heated to 500 °C at a rate of 5 °C/min. Next, the nanofibers were held at 500 °C for 2 h and then cooled to ambient temperature. In this step, the $CuAc_2$/PVA nanofibers were calcinated into Cu_xO nanofibers. To reduce the Cu_xO nanofibers to Cu nanofibers, the nanofibers were then heated in an atmosphere of hydrogen at a pressure of 40 Torr and flow rate of 200 sccm to 300 °C at 2 °C/min and held at 300 °C for 30 min.

Atomic Layer Deposition. The conformal AZO layers were coated at 150 °C using the Cambridge Nanotech Savannah with trimethyl aluminum (TMA), diethyl zinc (DEZ), and DI water as precursors. The pulse times for DEZ, TMA, and DI water were all 15 ms. A 20 nm thick AZO thin film was created by depositing 25 cycles of ZnO followed by 1 cycle of Al_2O_3 and then repeating this process four times. The molecular monolayers of Al precursors dope the ZnO to form a uniform AZO film. After the AZO film was deposited, another 10 cycles of Al_2O_3 was deposited to create a 1 nm layer of Al_2O_3.

Characterization. Gold contacts (180 nm thick) were coated onto the Cu nanofibers' transparent electrode using a thermal evaporator (MBraun). To reinforce the adhesion of the gold contact, a 7 nm layer of chromium was deposited before the gold deposition process. The pattern of gold contacts was designed to produce a square area of Cu nanofibers for sheet resistance measurement. Electrical measurements were performed using a multimeter, and the transmittance measurements

were conducted using an integrating sphere (Newport) and xenon lamp coupled with a monochromator. All transmittance measurements were referenced to a clear glass slide. Cu nanofibers were characterized by a SEM (FEI XL30 Sirion SEM, operating voltage 5 kV) and a TEM (FEI Tecnai G2 F20 X-TWIN with EDS, operating voltage 200 kV) equipped with EDS for chemical analysis.

Oxidation and Corrosion Testing. The thermal oxidation tests were performed in air using an oven (Fisher Scientific). Each sample was placed in the oven for various temperatures and time, removed from the oven, and allowed to equilibrate with the ambient temperature for 10 min. For the humidity testing, the humidity was measured and controlled by the hygrometer (Fisher Scientific) and oven (Barnstead Lab-line). For inorganic acid corrosion tests, the nanofibers were dipped into solutions with various pH values adjusted by KOH or HCl for 1 min and then rinsed with DI water twice to remove the residual etchant. The nanofibers were subsequently vacuum-dried for electrical measurement.

Conflict of Interest: The authors declare no competing financial interest.

Acknowledgment. P.-C.H. acknowledges the support from International Fulbright Science and Technology Award.

Supporting Information Available: Additional experimental details and figures. This material is available free of charge *via* the Internet at http://pubs.acs.org.

REFERENCES AND NOTES

1. Granqvist, C. G. Transparent Conductors as Solar Energy Materials: A Panoramic Review. *Sol. Energy Mater. Sol. Cells* **2007**, *91*, 1529–1598.
2. Hilsum, C. Flat-Panel Electronic Displays: A Triumph of Physics, Chemistry and Engineering. *Philos. Trans. R. Soc., A* **2010**, *368*, 1027–1082.
3. Hecht, D. S.; Hu, L. B.; Irvin, G. Emerging Transparent Electrodes Based on Thin Films of Carbon Nanotubes, Graphene, and Metallic Nanostructures. *Adv. Mater.* **2011**, *23*, 1482–1513.
4. Cairns, D. R.; Witte, R. P.; Sparacin, D. K.; Sachsman, S. M.; Paine, D. C.; Crawford, G. P.; Newton, R. R. Strain-Dependent Electrical Resistance of Tin-Doped Indium Oxide on Polymer Substrates. *Appl. Phys. Lett.* **2000**, *76*, 1425–1427.
5. *Mineral Commodity Summaries*. U.S. Geological Society, **2011**; p 74.
6. Yang, Y.; Heeger, A. J. Polyaniline as a Transparent Electrode for Polymer Light-Emitting-Diodes - Lower Operating Voltage and Higher Efficiency. *Appl. Phys. Lett.* **1994**, *64*, 1245–1247.
7. Wu, Z. C.; Chen, Z. H.; Du, X.; Logan, J. M.; Sippel, J.; Nikolou, M.; Kamaras, K.; Reynolds, J. R.; Tanner, D. B.; Hebard, A. F.; *et al.* Transparent, Conductive Carbon Nanotube Films. *Science* **2004**, *305*, 1273–1276.
8. Kim, K. S.; Zhao, Y.; Jang, H.; Lee, S. Y.; Kim, J. M.; Kim, K. S.; Ahn, J. H.; Kim, P.; Choi, J. Y.; Hong, B. H. Large-Scale Pattern Growth of Graphene Films for Stretchable Transparent Electrodes. *Nature* **2009**, *457*, 706–710.
9. Lee, J. Y.; Connor, S. T.; Cui, Y.; Peumans, P. Solution-Processed Metal Nanowire Mesh Transparent Electrodes. *Nano Lett.* **2008**, *8*, 689–692.
10. Wu, H.; Hu, L. B.; Rowell, M. W.; Kong, D. S.; Cha, J. J.; McDonough, J. R.; Zhu, J.; Yang, Y. A.; McGehee, M. D.; Cui, Y. Electrospun Metal Nanofiber Webs as High-Performance Transparent Electrode. *Nano Lett.* **2010**, *10*, 4242–4248.
11. Kim, K. K.; Reina, A.; Shi, Y. M.; Park, H.; Li, L. J.; Lee, Y. H.; Kong, J. Enhancing the Conductivity of Transparent Graphene Films *via* Doping. *Nanotechnology* **2010**, *21*, 285205.
12. Cui, Y.; Hu, L. B.; Kim, H. S.; Lee, J. Y.; Peumans, P. Scalable Coating and Properties of Transparent, Flexible, Silver Nanowire Electrodes. *ACS Nano* **2010**, *4*, 2955–2963.
13. Leskela, M.; Ritala, M. Atomic Layer Deposition Chemistry: Recent Developments and Future Challenges. *Angew. Chem., Int. Ed.* **2003**, *42*, 5548–5554.
14. Elam, J. W.; Routkevitch, D.; Mardilovich, P. P.; George, S. M. Conformal Coating on Ultrahigh-Aspect-Ratio Nanopores of Anodic Alumina by Atomic Layer Deposition. *Chem. Mater.* **2003**, *15*, 3507–3517.
15. Hong, S. S.; Cha, J. J.; Cui, Y. One Nanometer Resolution Electrical Probe *via* Atomic Metal Filament Formation. *Nano Lett.* **2011**, *11*, 231–235.
16. Greiner, A.; Wendorff, J. H. Electrospinning: A Fascinating Method for the Preparation of Ultrathin Fibres. *Angew. Chem., Int. Ed.* **2007**, *46*, 5670–5703.
17. Taylor, G. Disintegration of Water Drops in Electric Field. *Proc. R. Soc. London, Ser. A* **1964**, *280*, 383–397.
18. Deitzel, J. M.; Kleinmeyer, J.; Harris, D.; Tan, N. C. B. The Effect of Processing Variables on the Morphology of Electrospun Nanofibers and Textiles. *Polymer* **2001**, *42*, 261–272.
19. Hou, H. Q.; Reneker, D. H. Carbon Nanotubes on Carbon Nanofibers: A Novel Structure Based on Electrospun Polymer Nanofibers. *Adv. Mater.* **2004**, *16*, 69–73.
20. Wu, H.; Zhang, R.; Liu, X. X.; Lin, D. D.; Pan, W. Electrospinning of Fe, Co, and Ni Nanofibers: Synthesis, Assembly, and Magnetic Properties. *Chem. Mater.* **2007**, *19*, 3506–3511.
21. Dai, H. Q.; Gong, J.; Kim, H.; Lee, D. A Novel Method for Preparing Ultra-fine Alumina-Borate Oxide Fibres *via* an Electrospinning Technique. *Nanotechnology* **2002**, *13*, 674–677.
22. Sen, R.; Zhao, B.; Perea, D.; Itkis, M. E.; Hu, H.; Love, J.; Bekyarova, E.; Haddon, R. C. Preparation of Single-Walled Carbon Nanotube Reinforced Polystyrene and Polyurethane Nanofibers and Membranes by Electrospinning. *Nano Lett.* **2004**, *4*, 459–464.
23. Yang, J. C.; Kolasa, B.; Gibson, J. M.; Yeadon, M. Self-Limiting Oxidation of Copper. *Appl. Phys. Lett.* **1998**, *73*, 2841–2843.
24. George, S. M. Atomic Layer Deposition: An Overview. *Chem. Rev.* **2010**, *110*, 111–131.
25. Hu, L.; Hecht, D. S.; Gruner, G. Percolation in Transparent and Conducting Carbon Nanotube Networks. *Nano Lett.* **2004**, *4*, 2513–2517.
26. Haugsrud, R. The Influence of Water Vapor on the Oxidation of Copper at Intermediate Temperatures. *J. Electrochem. Soc.* **2002**, *149*, B14–B21.
27. Chang, Y.; Lye, M. L.; Zeng, H. C. Large-Scale Synthesis of High-Quality Ultralong Copper Nanowires. *Langmuir* **2005**, *21*, 3746–3748.
28. Sharma, S. P. Adsorption of Water on Copper and Cuprous Oxide. *J. Vac. Sci. Technol.* **1979**, *16*, 1557–1559.
29. Ni, J.; Yan, H.; Wang, A. C.; Yang, Y.; Stern, C. L.; Metz, A. W.; Jin, S.; Wang, L.; Marks, T. J.; Ireland, J. R.; *et al.* MOCVD-Derived Highly Transparent, Conductive Zinc- and Tin-Doped Indium Oxide Thin Films: Precursor Synthesis, Metastable Phase Film Growth and Characterization, and Application as Anodes in Polymer Light-Emitting Diodes. *J. Am. Chem. Soc.* **2005**, *127*, 5613–5624.
30. Wu, S.; Han, S. H.; Zheng, Y. N.; Zheng, H.; Liu, N. L.; Wang, L.; Cao, Y.; Wang, J. A. pH-Neutral PEDOT:PSS as Hole Injection Layer in Polymer Light Emitting Diodes. *Org. Electron.* **2011**, *12*, 504–508.